Monitoring thermal cracking with coda wave interferometry

Alexandre Grêt[†], Roel Snieder[†], John Scales[†] & Mike Batzle[‡]
[†] *Department of Geophysics and Center for Wave Phenomena, Colorado School of Mines.*
[‡] *Department of Geophysics and Center for Petrophysics, Colorado School of Mines.*

ABSTRACT
The coda of a waveform consists of that part of the signal after the directly arriving phases. At late times the coda is dominated by multiply scattered waves. Small changes in a medium, which would have no detectable influence on the first arrivals, are amplified by the multiple scattering and may be seen readily in the coda. We have exploited ultrasonic coda waves to study non-linear temperature dependence of velocity in granite. This non-linearity is related to acoustic emissions during thermal cracking. There are many other possible applications of this *Coda Wave Interferometry* in geophysics, including dam and volcano monitoring, time-lapse reservoir characterization, and rock physics.

Key words: velocity estimation, coda wave, multiple scattering, time-lapse, rock physics, acoustic emissions

Introduction

Geophysicists investigate the structure of the subsurface by making indirect measurements on the surface and relating them to those predicted by theoretical earth models. The Earth, however, is a highly complex system, and we almost always have to simplify our models in order to make them computationally tractable. In many applications, this simplification means treating unmodeled physics as noise, with the result that information contained in the data is discarded. For seismic data, coda waves are the tail of a seismogram. (In music the coda is the concluding passage of a movement or composition (Latin cauda, tail).) In this study we use coda waves to make inferences about thermally induced changes in granite. Those waves are the multiple scattered waves that arrive much later than the major wave types such as P, S and surface waves. Geophysical applications based on coda waves include earthquake prediction (Aki, 1985; Sato, 1988), volcano monitoring (Aki, 2000; Fehler *et al.*, 1998) or monitoring of temporal changes in the subsurface (Chouet, 1979; Revenaugh, 1995)(see also (Aki & Chouet, 1975).)

Consider the following examples: in monitoring a nuclear waste disposal site, one is not primarily interested in imaging the site. However, it is critical to monitor temporal changes in the site. In recent years, applied geophysicists have spent much effort on time-lapse seismics to monitor hydrocarbon reservoirs during recovery operations. Hydrocarbons move in the subsurface, reservoir rocks are artificially fractured, water-oil horizons move and steam propagates through the reservoir (Lumley, 1995; Wang, 1997). The high sensitivity of coda waves to small perturbations of the medium, makes them a powerful tool to monitor these kinds of changes.

We present a laboratory experiment in which we monitor the change in velocity resulting from a temperature change in a sample of Elberton granite. We excite and record ultrasonic waves and extract the velocity change from the coda waves. The same experiment is repeated with an aluminum sample in order to exclude temperature effects on the measurement equipment. Furthermore, we monitor acoustic emissions that result from heating the granite sample and correlate them to non-linear changes in seismic velocity.

Introduction to Coda Wave Interferometry

Coda wave interferometry uses multiply scattered waves to detect temporal changes in a medium, by using the

multiple scattering medium as an interferometer. For a change in the wave velocity, for quasi-random perturbations of the point scatterer location, or for a change in the source location, we can estimate this perturbation from multiply scattered waves by a cross-correlation in the time domain (Snieder *et al.*, 2002). We refer to the waveform before the perturbation as the unperturbed signal, and to the waveform after the perturbation as the perturbed signal. The unperturbed wave-field can be written as a Feynman path summation over all possible paths P (Snieder, 1999):

$$u_{\rm unp}(t) = \sum_P A_P S(t - t_P), \tag{1}$$

where a path is defined as a sequence of scatterers encountered by the wave, t_P is the travel time along path P, A_P is the corresponding amplitude and $S(t)$ is the source wavelet. When the background velocity is perturbed, the dominant effect on the waveform arises from the change in the travel time τ of the wave that travels along each path:

$$u_{\rm per}(t) = \sum_P A_P S(t - t_P - \tau_P). \tag{2}$$

We can now compute the time-windowed correlation coefficient between the unperturbed and the perturbed signal from:

$$R^{(t,T)}(t_s) \equiv \frac{\int_{t-T}^{t+T} u_{\rm unp}(t')\, u_{\rm per}(t'+t_s)dt'}{(\int_{t-T}^{t+T} u^2_{\rm unp}(t')dt' \int_{t-T}^{t+T} u^2_{\rm per}(t')dt')^{\frac{1}{2}}}, \tag{3}$$

where the time window is centered at time t with duration $2T$ and t_s is the time shift used in the cross-correlation. When the perturbed and unperturbed wavefields defined by equations (1) and (2) are inserted into (3), double sums over all paths appear. The cross-terms with different paths ($P \neq P'$) are incoherent and average out to zero when the mean of the source signal vanishes. We can therefore approximate the time-windowed correlation coefficient by:

$$R^{(t,T)}(t_s) \approx \frac{\sum_{P(t,T)} A_P^2\, C(\tau_P - t_s)}{\sum_{P(t,T)} A_P^2\, C(0)}, \tag{4}$$

where the sum is taken over the paths with arrival times within the time window of the cross-correlation, and the auto-correlation of the source signal is defined as

$$C(t) \equiv \int_{-\infty}^{\infty} S(t'+t)S(t')dt'. \tag{5}$$

For time shifts τ much smaller than the dominant period, a second-order Taylor expansion gives $C(\tau) = C(0)(1 - \frac{1}{2}\overline{\omega}^2\tau^2)$, where $\overline{\omega}^2$ is the mean-squared frequency of the waves that arrive in the time window. Using this in equation (4) we can write

$$R^{(t,T)}(t_s) = 1 - \frac{1}{2}\overline{\omega}^2 \left\langle (\tau - t_s)^2 \right\rangle_{(t,T)}, \tag{6}$$

where $\langle \cdots \rangle_{(t,T)}$ stands for the average over the wave paths with arrivals in the time interval $(t-T, t+T)$.

The time shifted cross-correlation $R^{(t,T)}(t_s)$ has a maximum when

$$t_s = t_{\rm max} \equiv \langle \tau \rangle_{(t,T)}, \tag{7}$$

where $\langle \tau \rangle_{(t,T)}$ is the mean travel time perturbation of the arrivals in the time window. Using (6) and (7) gives the maximum value of the cross-correlation

$$R^{(t,T)}_{\rm max} = 1 - \frac{1}{2}\overline{\omega}^2\sigma^2_\tau, \tag{8}$$

where σ^2_τ is the variance of the travel time perturbation for waves arriving within the time window. This means that we can extract the mean and the variance of the travel time perturbations of the waves arriving in a time window.

For a constant change δv in seismic velocity and fixed locations of the scatterers, the mean travel time perturbation is given by $\langle \tau \rangle_{(t,T)} = -(\delta v/v)t$. When the time window is small ($T \ll t$), $\sigma_\tau = 0$. The velocity change follows from the time of the maximum of the time-shifted cross-correlation function:

$$\frac{\delta v}{v} = \frac{t_{max}}{t}. \tag{9}$$

Other types of perturbations leave a different signature on the time shifted correlation coefficient (Snieder *et al.*, 2002).

Monitoring Thermally Induced Velocity Changes with Coda Wave Interferometry

In the ultrasonic experiment we first use an aluminum cylinder with a hight of 11 cm and a diameter of 5.5 cm. The sample is equipped with a sonic source on one side and a receiver on the other (Figure 1). The transducer sends a pulse through the sample and the single receiver, records the impulse response of the sample, with a sampling interval of 1μs (the dominant frequency is 100 kHz.) Ten traces are stacked to reduce the noise level. Two typical records for a cylindrical sample are shown in Figure 2.

To apply a controlled change in the medium over time, the aluminum sample is equipped with a heating element in a central borehole. The temperature is monitored by a thermocouple glued to the side of the sample (Figure 1).

While increasing the temperature from 25^oC to 90^oC, the sonic measurement is repeated for every 5^oC increase in temperature. Then the aluminum sample is cooled to room-temperature and the sonic experiment is repeated again for every 5^oC in temperature decrease. In addition, acoustic emissions are counted for every temperature interval.

In many laboratory experiments, the change in the seismic velocity is measured for a temperature change

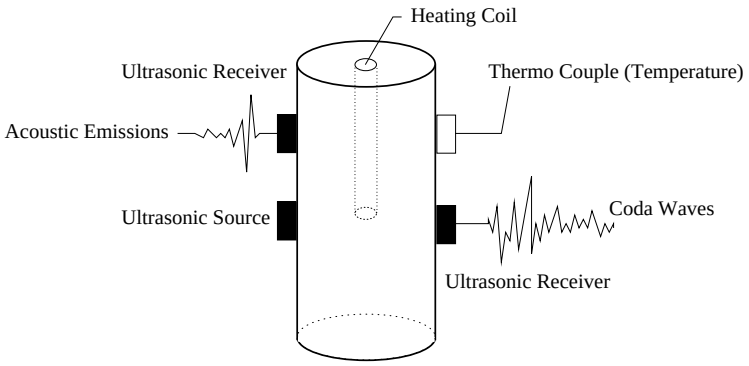

Figure 1. Experimental setup. The cylinder represents the Elberton granite or the aluminum sample. Sonic waves are transmitted through the sample. A longitudinal transducer, which excites primarily P-waves, and an identical receiver (right rectangle) are used throughout the experiment. A third identical P-wave transducer (top left rectangle) detects the acoustic emissions. The sample is heated with a heating coil placed in a centered borehole and the temperature is measured with a thermo-couple at the sample surface (white rectangle.)

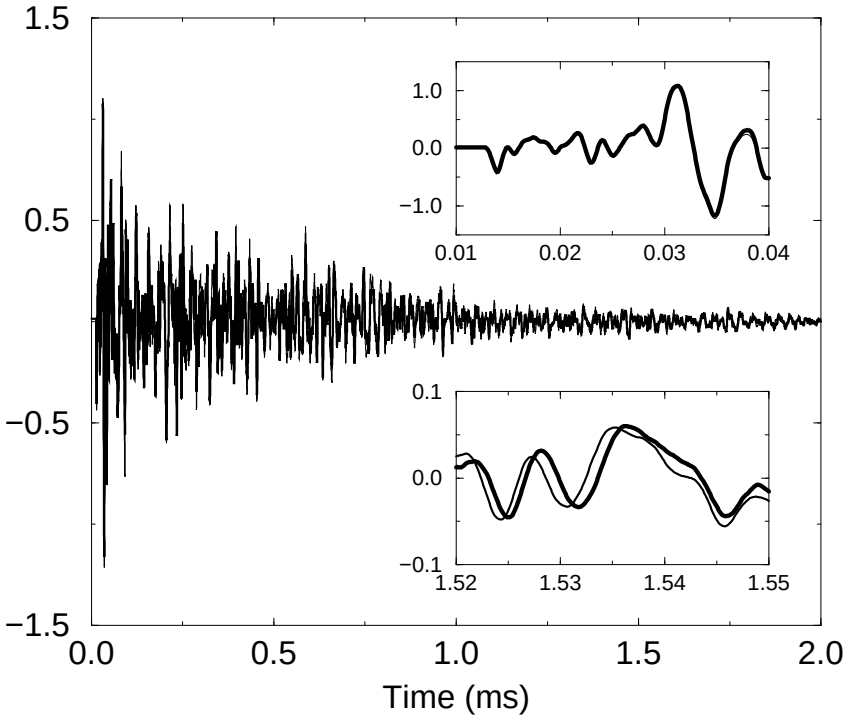

Figure 2. Wave-forms recorded in the granite sample for temperatures of 45^oC (thin) and 50^oC (thick) respectively. The insets show details of the wave-forms around the first arrival (top) and in the late coda (bottom.)

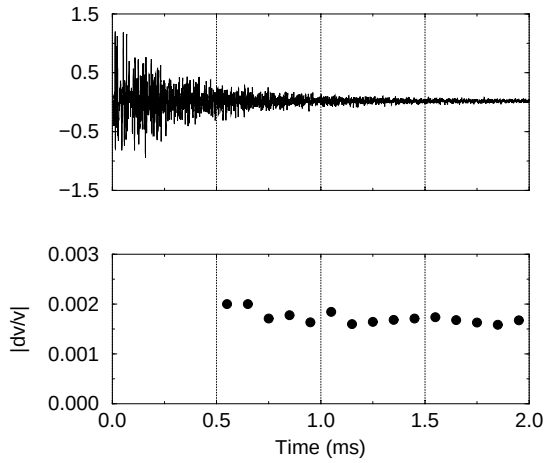

Figure 3. The top figure shows the ultra-sonic signal recorded on the aluminum sample. The bottom figure shows different estimates of $\delta v/v$ for multiple time-windows, therefore providing a consistency check. The early part of the signal is not used because it can't be considered a multiply scattered regime.

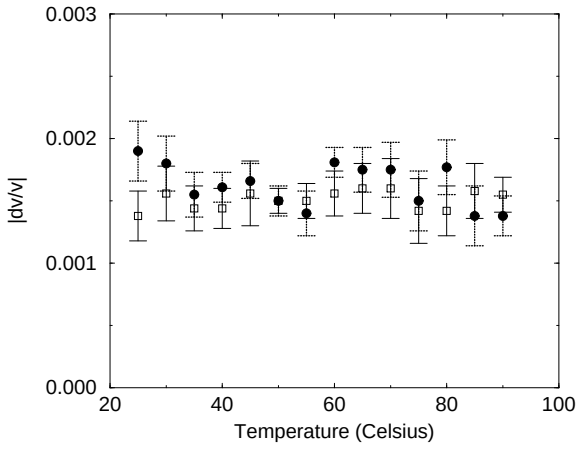

Figure 4. Absolute values of $\delta v/v$ in aluminum, for 5^oC temperature intervals from 25^oC to 90^oC. Circles correspond to the heating phase and rectangles (unfilled) to the cooling phase.

of about 100^oC (Kern *et al.*, 2001; Timur, 1977; Peselnick & Stewart, 1975; Hughes & Maurette, 1956). For a 11 cm small sample and a temperature difference of only 5^oC, there is no significant travel-time difference for the first arriving waves (see top inset of Figure 2). Therefore, first arriving waves do not provide any information about velocity changes. In a late time window (bottom inset of Figure 2), we see a distinct time shift of the wave-forms. This information can be used to infer the change of sonic velocity with temperature.

For each change of 5^oC in temperature the relative change in velocity is estimated from equation (9), with 20 different 0.1ms time windows of the coda waves. Every window provides an independent estimate of the relative velocity change, that can be used for a consistency check of the method (Figure 3). Since we have multiple estimates of $\delta v/v$ we can calculate the mean and variance of the relative velocity change. The relative velocity change is of the order of 0.15% for a temperature change of 5^oC with an error of 0.025% (Figure 4). It is important to note that the relative velocity change with temperature does not depend on whether the sample is in the heating or the cooling phase. Furthermore, there is no measurable velocity difference at room temperature before and after the sample has gone through the heating cycle.

This laboratory experiment is important to test the presence of temperature effects on the measurement equipment, like piezoelectric transducer, cables, transducer couplant or mounting devices. Since we measure a linear velocity change with temperature in aluminum, we conclude that these effects can be neglected.

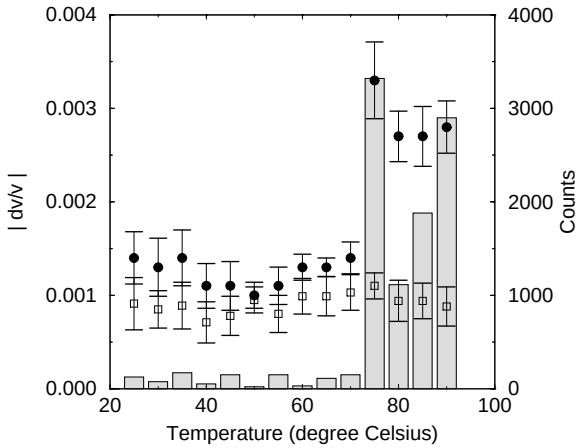

Figure 5. Absolute values of $\delta v/v$ in Elberton granite, for 5^oC temperature intervals from 25^oC to 90^oC. Circles correspond to the heating phase and rectangles to the cooling phase. The histograms show the count of acoustic emissions for a given temperature interval.

Monitoring Thermally Induced Velocity Change and Acoustic Emissions in Granite

With the same technique and same experimental setup described above, we measure the thermally induced velocity change in a granite sample. During the heating phase the velocity decrease for temperatures below 70^oC is constant, however for every 5^oC increase above that temperature, the velocity change increases (Figure 5). 70^oC corresponds to the critical fracture temperature

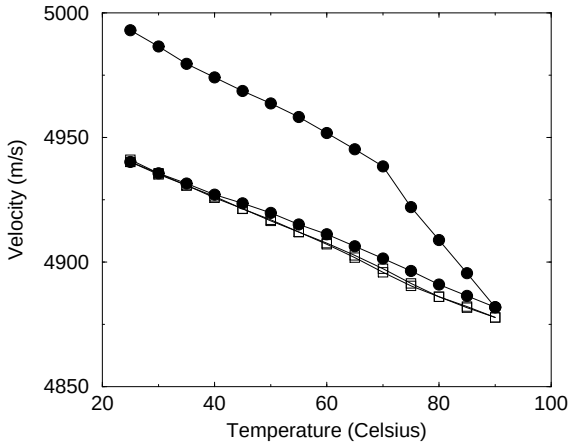

Figure 6. Absolute velocity versus temperature in Elberton granite, for two heating cycles. Filled circles represent the first heating cycle and rectangles the second. Note that on the second heating cycle the temperature dependent velocities during the heating and cooling phase are almost not distinguishable.

for granite (Johnson *et al.*, 1978; Fredrich & Wong, 1986). Thermal cracking results from the internal stress concentration induced by thermal expansion anisotropy or thermal expansion mismatch between minerals or grains. Such micro-cracking is a similar effect as the thermal stresses induced by thermal gradients in solids; for a high temperature gradient, cracking may occur even in a perfectly homogeneous solid (Boley & Weiner, 1960). Fredrich & Wong (1986) show that thermal cracking in rocks occurs principally along mineral or grain boundaries. The thermally induced cracks can influence significantly both the mechanical and transport properties, as well as thermoelastic moduli (Simmons & Cooper, 1978).

In addition to the experiment with the aluminum cylinder, we use a third ultrasonic transducer in order to detect acoustic emissions in the granite due to thermal cracking. Figure 5 shows the count of acoustic emissions versus temperature. There is a small amount of acoustic emissions at low temperatures. However, there is a significant increase in acoustic emissions between 70^oC and 75^oC. The increase in velocity change and the jump in the number of acoustic emissions correlate well.

Irreversible Change in Velocity Due to Thermal Cracking

In the 1930's, Kaiser found that during repeated loading of metals, little or no acoustic emissions occurred until previously applied stress levels where exceeded. Since then, this effect has been known as the "Kaiser effect". Later, it was found that the Kaiser effect is a common phenomenon for various materials including rocks (Kurita & Fujii, 1979). Thus, the maximum stress applied in the previous cycles is 'memorized' in rocks.

During the cooling phase of the granite, there is no non-linear velocity change at 70^oC and there is only few acoustic emissions over the entire period. The seismic velocity does not increase back to its initial value. This difference in velocity is due to irreversible damage done to the rock by thermal cracking (Figure 6).

Todd (1973) studied the acoustic emissions of Westerly granite during cyclic heating. He noted that if a sample was re-heated to the same maximum temperature, few acoustic emissions occurred. Similarly we find in a second heating cycle up to the same maximum temperature (90^oC) for the same granite sample, only few acoustic emissions events occur and there is no non-linear velocity decrease around 70^oC. Furthermore, the velocity increases back to the value before the second heating cycle when cooled down (Figure 6). Note, that there is a small difference in relative velocity change between the cooling phase of the first heating cycle and the second cycle. Thirumalai & Demou (1973) studied the residual strain in a granitic rock produced by cyclic heating, and showed that predominant damage took place during the initial exposure to heating and the damage reached a steady state after three successive heating cycles.

This indicates that two different mechanisms drive the temperature induced velocity change. The first mechanism is the change in bulk elastic constants with temperature, which is linear and reversible. This explains the constant velocity change with temperature during the second heating cycle during heating and cooling. The second mechanism is the damage done to the granite due to thermal cracking, which explains the non-linear velocity change at the critical fracture temperature during the first heating cycle.

In 1937 Ide found the same temperature dependance of velocity in Quincy granite. By means of first arrival travel time, he optained 7 measurments over one heating cycle, with a peak temperature of 300^oC. With Coda Wave Interferometry we are able to measure twenty times more points over the same temperature intervall.

Conclusions

Due to the extreme sensitivity of coda wave interferometry, we are able to study temperature effects on small rock samples to a high level of precision. It is often assumed that seismic velocity depends linearly on temperature up to a temperature of about 300^oC. We show that under laboratory conditions (atmospheric pressure, unconfined sample), this is not the case. Furthermore, we can relate the non-linearity to thermal cracking.

The velocity estimation based on the coda waves

requires only a single repeatable source and a single receiver. This means that one can monitor minute changes in-situ. The laboratory experiment is closely related to important problems in nuclear waste deposits, where thermally induced cracking allows contaminated fluids to move around. In coda wave interferometry we have a technique to monitor a nuclear waste deposit in an inexpensive, automated and precise way. It might also be used, for example, as a diagnostic for non-destructive testing, volcano monitoring, or monitoring of hydrocarbon reservoirs.

Acknowledgments

We thank Dr. Robert Krantz for his help and advice. The original manuscript has much improved with suggestions from Dr. Luis Tenorio. This work was partially supported by the NSF(EAR-0106668 and EAR-0111804), by the US Army Research Office (DAAG55-98-1-0070), and by the sponsors of the Consortium Project on Seismic Inverse Methods for Complex Structures at the Center for Wave Phenomena.

REFERENCES

Aki, K. 1985. Theory of earthquake prediction with special reference to monitoring of the quality factor of lithosphere by the coda method. *Earthquake Res. Bull.*, **3**, 219–230.

Aki, K. 2000. Seismic monitoring and modeling of an active volcano for prediction. *J. Geophys. Res.*

Aki, K., & Chouet, B. 1975. Origin of Coda Waves: Source, Attenuation, and Scattering Effects. *J. Geophys. Res.*

Boley, B.A., & Weiner, J.H. 1960. *Theory of Thermal Stresses.* New York.

Chouet, B. 1979. Temporal variation in the attenuation of earthquake coda near Stone Canyon, California. *Geophys. Res. Lett.*, **6**, 143–146.

Fehler, M., Roberts, P., & Fairbanks, T. 1998. A temporal change in coda wave attenuation observed during an eruption of Mount St. Helens. *J. Geophys. Res.*, **93**, 4367–4373.

Fredrich, J.T., & Wong, T. 1986. Micromechanics of thermally induced cracking in three crustal rocks. *J. Geophys. Res.*, **91**, 12743–12764.

Hughes, D.S., & Maurette, C. 1956. Variation of elastic wave velocities in granites with pressure and temperature. *Geophysics*, **21**, 277–284.

Johnson, B., Gangi, A.F., & Handin, J. 1978. Thermal cracking subjected to slow, uniform temperature changes. *paper presented at 19th U.S. Rock Mechanics Symposium, U.S. Nat. Comm. for Rock Mech., Univ. of Nevada, Reno.*

Kern, H., Popp, T., Gorbatsevich, F., Zkarikov, A., Labanov, K.V., & Smirnov, Yu.P. 2001. Pressure and temperature dependence of V_P and V_S in rocks from the superdeep well and from surface analogues at Kola and the nature of velocity anisotropy. *Tectonophysics*, **338**, 113–134.

Kurita, K., & Fujii, N. 1979. Stress memory of crystalline rocks in acoustic emission. *Geophys. Res. Letters.*

Lumley, D.E. 1995. *Seismic time-lapse monitoring of subsurface fluid flow.* Ph.D. thesis, Stanford Univ.

Peselnick, L., & Stewart, R.M. 1975. A sample assembly for velocity measurements of rocks at elevated temperatures and pressures. *J. Geophys. Res.*, **80**, 3765–3768.

Revenaugh, J. 1995. The Contribution of Topographic Scattering to Teleseismic Coda in Southern California. *Geophys. Res. Lett.*, **22**, 543–546.

Sato, H. 1988. Temporal change in scattering and attenuation associated with the earthquake occurence - a review of recent studies on coda waves. *Pure Appl. Geophy.*, **126**, 465–497.

Simmons, G., & Cooper, H.W. 1978. Thermal cycling cracks in three igneous rocks. *Int. J. Rock Mech.*

Snieder, R. 1999. Imaging and Averaging in Complex Media. *Pages 405–454 of:* Fouque, J.P. (ed), *Diffuse waves in complex media.* Dordrecht: Kluwer.

Snieder, R., Grêt, A., Douma, H., & Scales, J. 2002. Coda Wave Interferometry for Estimating Nonlinear Behavior in Seismic Velocity. *Science*, **295**, 2253–2255.

Thirumalai, K., & Demou, S.G. 1973. Thermal expansion behaviour of intact and thermal fractured mine rocks. *Am. Inst. Phys. Conf. Proc.*

Timur, A. 1977. Temperature dependence of compressional and shear wave velocities in rocks. *Geophysics*, **42**, 950–956.

Todd, T.P. 1973. Effects of cracks on elastic properties of low porosity rocks. *Thesis, Massachusetts Institute of Technology.*

Wang, Z. 1997. Feasibility of time-lapse seismic reservoir monitoring: The physical basis. *The Leading Edge.*